

KUNS-1209  
 HE(TH) 93/06  
 hep-ph/9307365  
 July, 1993

# Interpolating Axial Anomaly Induced Amplitudes

Masako BANDO\* and Masayasu HARADA†

*Department of Physics, Kyoto University,  
 Kyoto 606-01, Japan*

## Abstract

We propose an interpolating formula for the amplitude induced by the axial anomaly, concentrating on the  $\pi^0\gamma^*\gamma^*$  transition form factor. The QCD corrections to this amplitude are generally described by two major contributions coming from the  $q\bar{q}$  bound state and the background continuous spectrum, respectively.

For the first contribution, we include the lowest vector bound state using the realization of the dynamical gauge boson of hidden local symmetry. The second contribution is included as the triangle quark loop in which a constituent mass is adopted as a internal quark mass and the amplitudes are smeared out around the threshold. Using the resulting form factor, we fit the experimental data for the  $\pi^0\gamma$  and the  $\omega\pi^0$  transition form factors and show that our result describes the experimental data well.

---

\*Permanent address: Aichi University, Miyoshi Aichi 470-02, Japan

†Fellow of the Japan Society for the Promotion of Science for Japanese Junior Scientists

# 1 Introduction

The non-Abelian anomaly is one of the most prominent features of quantum gauge theories, and it has provided us with important information on the matter content of gauge theories. In particular the well-studied  $\pi^0 \rightarrow \gamma\gamma$  process, which is controlled by the axial anomaly, gave the first clear indication of the physical existence of the color degrees of freedom in the quark model.

As is well known, a low energy effective chiral Lagrangian may be written in terms of the Nambu Goldstone (NG) bosons: this Lagrangian is based on the nonlinear realization of the chiral symmetry of QCD. All relevant anomaly terms must be taken into account in this low energy effective chiral Lagrangian. This is done by introducing Wess-Zumino terms[1, 2],  $\mathcal{L}_{WZ}$ , which determine exactly the scattering amplitudes in the zero momentum limit (the low energy theorem[3, 4, 5]). The values of the anomaly terms are determined by calculating the well-known fermion triangle graph of Fig. 1. The value of the amplitude in the low energy limit does not depend on either the higher order corrections or the internal fermion masses.

If one wants to extend the Lagrangian to a small but nonzero energy scale, one should also include the non-anomalous terms, and incorporate the QCD corrections to this triangle graph into the effective Lagrangian. The QCD effects are represented as a rich spectrum of intermediate states in each channel. Those may be quite well described by the following two major contributions: the first is a variety of quark-antiquark bound states (hadrons) which come into the amplitudes as poles in each channel and the second is a continuous spectrum which contributes to the background amplitudes.

The most important candidates for the bound states are the non NG boson low-mass states, i.e., the vector mesons. It is known that the easiest way to include these in a consistent and systematic formulation is to treat them in the framework of dynamical realization of hidden local symmetry[6]. In this section the vector mesons are introduced in the effective Lagrangian without any mismatch to the low energy theorem. The second effect may be well modeled by including the triangle quark one-loop contributions. In calculating these, however, one should adopt the non-perturbative “constituent quark masses” instead of the current quark masses. The calculation should also be smeared out around the  $q\bar{q}$  threshold because quarks are confined and multi-hadron (pion) threshold effects arise instead of multi-quarks.

On the other hand, the asymptotic freedom of QCD facilitates us to predict the hadronic amplitudes in the extremely high energy region, where again the triangle diagram becomes

dominant. The contributions have been extensively studied[7, 8] in connection with deep scattering exclusive processes. The high energy behavior is obtained almost exactly up to an ambiguity in the coefficient factor. Thus it is important to notice that the anomaly induced amplitudes are constrained not only by the low energy theorem but also by the high energy behavior.

In this paper we propose an interpolating formula for the anomaly induced amplitudes which matches the behaviors in both the low and high energy limits. We focus on the electromagnetic pion transition form factor as an example, and check our interpolating formula reproduces the existing experimental data.

This paper is organized as follows. Section 2 is devoted to the formulation and the presentation of the basic tools for computing the anomaly induced decay amplitudes and the corresponding form factors. In section 3, the quark triangle graph is studied, and we propose how to take account of QCD corrections. Section 4 is devoted to a review of the hidden local symmetry model and discussions on the low energy form factor including the effects of the vector mesons. In sect. 5 we propose the interpolating form factors. In sect. 6 we fit our form factor with the experimental data for the  $\pi^0\gamma$  transition form factor and give the  $Z \rightarrow \pi^0\gamma$  decay width. In sects. 7 and 8 we study the  $\omega\pi^0$  transition form factor and its related processes to check the validity of our form factor. Section 9 contains summary and discussions.

## 2 Definition

Let us start with the anomalous Ward-Takahashi identity:

$$\partial_\mu j_5^\mu = 2m_0 j_5 + \frac{e^2}{16\pi^2} F\tilde{F}, \quad (2.1)$$

where  $j_5^\mu$  is the axial-vector current\* which generally couples to NG bosons, and  $j_5$  is the corresponding pseudoscalar density. In particular, for the  $\pi^0$  case,  $j_5^\mu = \sum_i \bar{q}_i T_i \gamma^\mu \gamma_5 q_i$ ,  $q_i = (u, d)$ ,  $T_i = (1/2, -1/2)$ , and  $2m_0 j_5 \equiv \sum_i 2m_{0i} \bar{q}_i T_i i \gamma_5 q_i$ , where  $m_{0i}$  is the current quark mass. Hereafter, we shall take as an example the case in which  $j_5^\mu$  couples to  $\pi^0$  to demonstrate the concrete forms of the amplitudes, although general expressions can be obtained straightforwardly. In the  $\pi^0$  case, only the  $u$  and  $d$  quarks come into play.

We consider the following three-point function:

$$T^{AB,\mu\nu\rho}(p, q) = -i \int d^4x d^4y e^{-ik\cdot y + ip\cdot x} \langle 0 | T j^{A\nu}(x) j^{B\rho}(0) j_5^\mu(y) | 0 \rangle, \quad (2.2)$$

---

\*Here we restrict ourselves to neutral currents.

where  $q \equiv k - p$ , and  $j^{A\nu}(x)$  and  $j^{B\rho}(0)$  are the vector currents,  $j^{A\nu} = \sum_i \bar{q}_i Q_i^A \gamma^\nu q_i$  with  $Q_i^A$  being the vector charge of the  $i$ th quark  $q_i$ . (The suffices  $A$  and  $B$  run over  $\gamma$ ,  $Z$ ,  $\dots$ , etc., depending on the gauge field to which the current couples. The normalization of  $Q^A$  is determined so that the coupling between the current and the gauge field is given by  $e j^{A\mu} A_\mu$ .)

PCAC in the presence of the anomaly gives the following relation[9, 10]:

$$k_\mu T^{AB,\mu\nu\rho}(p, q) = M^{AB,\mu\nu}(p, q) + \frac{N_c e^2}{4\pi^2} \text{tr} \left\langle T \left\{ Q^A, Q^B \right\} \right\rangle \varepsilon^{\alpha\beta\nu\rho} p_\alpha q_\beta, \quad (2.3)$$

where  $N_c (= 3)$  is the number of colors, and

$$M^{AB,\nu\rho}(p, q) = -f_P m_P^2 \int d^4x d^4y \exp(ip \cdot x) \exp(-ik \cdot y) \langle 0 | T j^{A\nu}(x) j^{B\rho}(0) \phi_P(y) | 0 \rangle \quad (2.4)$$

represents the anomaly induced amplitude for the NG boson,  $\phi_P(y)$ , to couple to vector currents  $j^{A\nu}$  and  $j^{B\rho}$ . If one defines the following function  $T(p^2, q^2, k^2)$ :

$$M^{AB,\nu\rho}(p, q) \equiv -\frac{N_c e^2}{4\pi^2 f_P} \text{tr} \left\langle T \left\{ Q^A, Q^B \right\} \right\rangle \varepsilon^{\alpha\beta\nu\rho} p_\alpha q_\beta T(p^2, q^2, k^2), \quad (2.5)$$

this function  $T(p^2, q^2, k^2)$  determines the axial anomaly induced amplitude. In the low energy limit this is determined exactly by the low energy theorem. The  $k^2 = 0$  limit of the function  $T(p^2, q^2, k^2)$  for  $\pi^0$  case determines the  $\pi^0 \gamma^* \gamma^*$  transition form factor:

$$F(\pi^0, \gamma(p^2), \gamma(q^2)) = T(p^2, q^2, k^2 = 0). \quad (2.6)$$

The low energy theorem requires the following normalization of this form factor:

$$F(\pi^0, \gamma(p^2 = 0), \gamma(q^2 = 0)) = 1. \quad (2.7)$$

It is our purpose to investigate the properties of  $T(p^2, q^2, k^2)$  not only in the low energy limit but also in the high energy region where  $p^2$  or  $q^2$  is large.

### 3 Triangle Anomaly Graph and QCD Corrections

#### 3.1 Triangle Quark One-Loop Graph

The quark triangle graph shown in Fig. 1 gives the main contribution to the LHS of Eq.(2.3) This is evaluated as

$$\begin{aligned} & k_\mu T^{AB,\mu\nu\rho}(p, q) \Big|_{\text{triangle}} \\ &= \frac{N_c e^2}{4\pi^2 f_\pi} 2 \sum_i T_i Q_i^A Q_i^B \varepsilon^{\alpha\beta\nu\rho} p_\alpha q_\beta \left[ 1 - \int [dz] \frac{m_i^2}{m_i^2 - z_2 z_3 k^2 - z_3 z_1 p^2 - z_1 z_2 q^2} \right], \end{aligned} \quad (3.1)$$

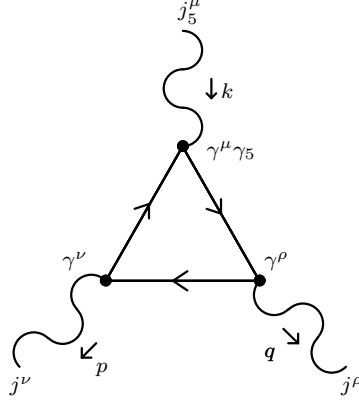


Figure 1: The quark triangle anomaly graph

where  $m_i$  is the  $i$ th quark mass,  $f_\pi = 93\text{MeV}$  is the pion decay constant and the Feynman parameter integral is defined by

$$\int [dz] \equiv 2 \int_0^1 dz_1 dz_2 dz_3 \delta(1 - z_1 - z_2 - z_3). \quad (3.2)$$

Thus, we get

$$T(p^2, q^2, k^2) \Big|_{\text{triangle}} = \frac{2 \sum_i T_i Q_i^A Q_i^B}{\text{tr} \langle T \{Q^A, Q^B\} \rangle} \int [dz] \frac{m_i^2}{m_i^2 - z_2 z_3 k^2 - z_3 z_1 p^2 - z_1 z_2 q^2}. \quad (3.3)$$

It is easy to see that in the low energy limit in which  $k^2 = p^2 = q^2 = 0$ , this reduces to

$$T(p^2 = 0, q^2 = 0, k^2 = 0) \Big|_{\text{triangle}} = 1, \quad (3.4)$$

independently of  $m_i$ . This is of course because the anomaly term is exactly reproduced by the lowest order triangle graph. Here we define the triangle graph contributions to  $T(p^2, q^2, k^2 = 0)$ :

$$I(p^2, q^2) \equiv T(p^2, q^2, k^2 = 0) \Big|_{\text{triangle}}. \quad (3.5)$$

Let us study the high energy behavior of this function. After performing the parameter integration we obtain

$$\begin{aligned} I(p^2, q^2) &= \frac{2 \sum_i T_i Q_i^A Q_i^B}{\text{tr} \langle T \{Q^A, Q^B\} \rangle} \\ &\times \frac{m_i^2}{p^2 - q^2} \left[ \left\{ \ln \frac{\sqrt{4m_i^2 - q^2} + \sqrt{-q^2}}{\sqrt{4m_i^2 - q^2} - \sqrt{-q^2}} \right\}^2 - \left\{ \ln \frac{\sqrt{4m_i^2 - p^2} + \sqrt{-p^2}}{\sqrt{4m_i^2 - p^2} - \sqrt{-p^2}} \right\}^2 \right]. \end{aligned} \quad (3.6)$$

For the  $\pi^0$  case, we take  $m_u \simeq m_d = m$  and get

$$I(p^2, q^2) = \int [dz] \frac{m^2}{m^2 - z_3 z_1 p^2 - z_1 z_2 q^2}, \quad (3.7)$$

whose high energy behavior is given by

$$I(p^2 \gg m^2, q^2 \gg m^2) \simeq \frac{m^2}{p^2 - q^2} \left[ \left\{ \ln \frac{m^2}{q^2} + i\pi \right\}^2 - \left\{ \ln \frac{m^2}{p^2} + i\pi \right\}^2 \right]. \quad (3.8)$$

If one photon is on its mass shell (e.g.,  $p^2 = 0$ ), then the function  $I(p^2, q^2)$  reduces to

$$\begin{aligned} J(q^2) &\equiv I(p^2 = 0, q^2) \\ &= -\frac{m^2}{q^2} \left[ \left\{ \ln \frac{\sqrt{4m^2 - q^2} + \sqrt{-q^2}}{\sqrt{4m^2 - q^2} - \sqrt{-q^2}} \right\}^2 \right], \end{aligned} \quad (3.9)$$

which gives the  $\pi^0\gamma$  transition form factor. The high energy behavior of this function is given by

$$J(q^2 \gg m^2) \simeq \frac{m^2}{q^2} \left[ \pi^2 - \left( \ln \frac{m^2}{q^2} \right)^2 - 2i\pi \ln \frac{m^2}{q^2} \right]. \quad (3.10)$$

As we shall see later, this form factor, with the constituent quark mass used in place of the current quark mass, is consistent with the short range behavior obtained from the operator product expansion (OPE) technique[7, 11]. In the intermediate region, however, we have to take account of the higher order corrections, especially, the QCD effects can not be neglected.

## 3.2 QCD Corrections to Quark Triangle Anomaly Graph

It is well known that, in the low energy limit, the higher order corrections do not change the value of the anomaly induced three-point function in Eq.(2.2), or  $T(p^2 = q^2 = k^2 = 0)$  itself. However, higher order corrections do contribute appreciably to its higher energy behavior.

Generally QCD effects are represented as a rich hadron spectrum, with the most important contributions coming from the lowest energy bound states, i.e. the vector mesons. This can be elegantly described in the framework of hidden local symmetry, which will be briefly summarized in the section 4. All other QCD effects, including the higher resonances with broader widths, are expressed as a background amplitude. This background amplitude may be reasonably well described by the triangle quark contributions of Fig. 1, in which, however, one should include the following two kinds of major non-perturbative QCD effects: 1) the current quark masses should be replaced by the constituent quark masses; 2) the amplitude should be smeared out around the  $q\bar{q}$  threshold.

1) Since the chiral symmetry has been spontaneously broken and there appear NG bosons, the quarks necessarily acquire dynamical masses. Thus, in this phase of broken

chiral symmetry, it is natural to replace the current quark mass by the constituent quark mass in the function  $I(p^2, q^2)$ . Note that, however, this replacement never changes the value of the low energy limit, because  $I(p^2 = 0, q^2 = 0) = 1$  independently of the quark mass (see Eq.(3.4)). Further, the asymptotic behavior of  $I(p^2 = 0, q^2) = 1$  at large  $q^2$  has been found to be of order  $\mathcal{O}(m^2/q^2)$ , which is almost consistent with the short range behavior obtained from the OPE[7, 11], because the constituent quark masses are of order  $f_\pi$  (note that in the chiral limit use of  $m = 0$  gives completely the wrong behavior.) It is the asymptotic freedom of QCD that guarantees the validity of the perturbative expansion at short distance. As a result the triangle graph becomes dominant.

2) The graph in Fig. 1 shows the contribution of the  $q\bar{q}$  threshold at  $p^2 = 4m^2$  ( $q^2 = 4m^2$ ) from which an imaginary part emerges as shown in Fig. 2 (the dotted lines). However, since the quarks are confined, the intermediate states are not multi-quark states but actually multi-hadron states ( $2\pi$ ,  $4\pi$ , ... etc.). The above effect may be properly taken into account by smearing out the original  $J(q^2)$ . Here we adopt the following function:

$$\tilde{J}(x) \equiv -\frac{(\ln(1+x))^2}{x} + \frac{\ln(1+x)}{x} + \alpha x \exp(-\beta x) + 2\pi i \frac{\ln(1+x)}{x} \exp\left(-\frac{\lambda}{x}\right), \quad (3.11)$$

where  $x = q^2/m^2$ . Both  $J$  and  $\tilde{J}$  are shown in Fig. 2, where we take the parameter choice  $\alpha = 1.4$ ,  $\beta = 0.35$  and  $\lambda = 2.5$ . From this figure, we see that the modified amplitudes  $\tilde{J}$  are properly smeared out. This form has been chosen so as to coincide with the original  $J$  (the dotted lines) both in the high and low energy limits.

## 4 Hidden Local Symmetry and Vector Mesons

In order to get the full amplitude, we need further to take account of the dominant resonances, which in our case are the vector meson poles in the relatively low energy region. This can be done consistently and systematically in the framework of hidden local symmetry (HLS)[12].

### 4.1 Hidden Local Symmetry

First, following Ref.[6], we briefly review hidden local symmetry. In this framework the vector mesons are introduced as the dynamical gauge bosons of hidden local symmetry[13].

For the case of the  $\pi^0$  form factor, the low energy QCD system is known to be described by the model based on the manifold  $G/H = U(2)_L \times U(2)_R/U(2)_V$ <sup>†</sup>. The low energy

---

<sup>†</sup>We have to take account of gluon anomaly in the case of  $\eta$  and  $\eta'$ .

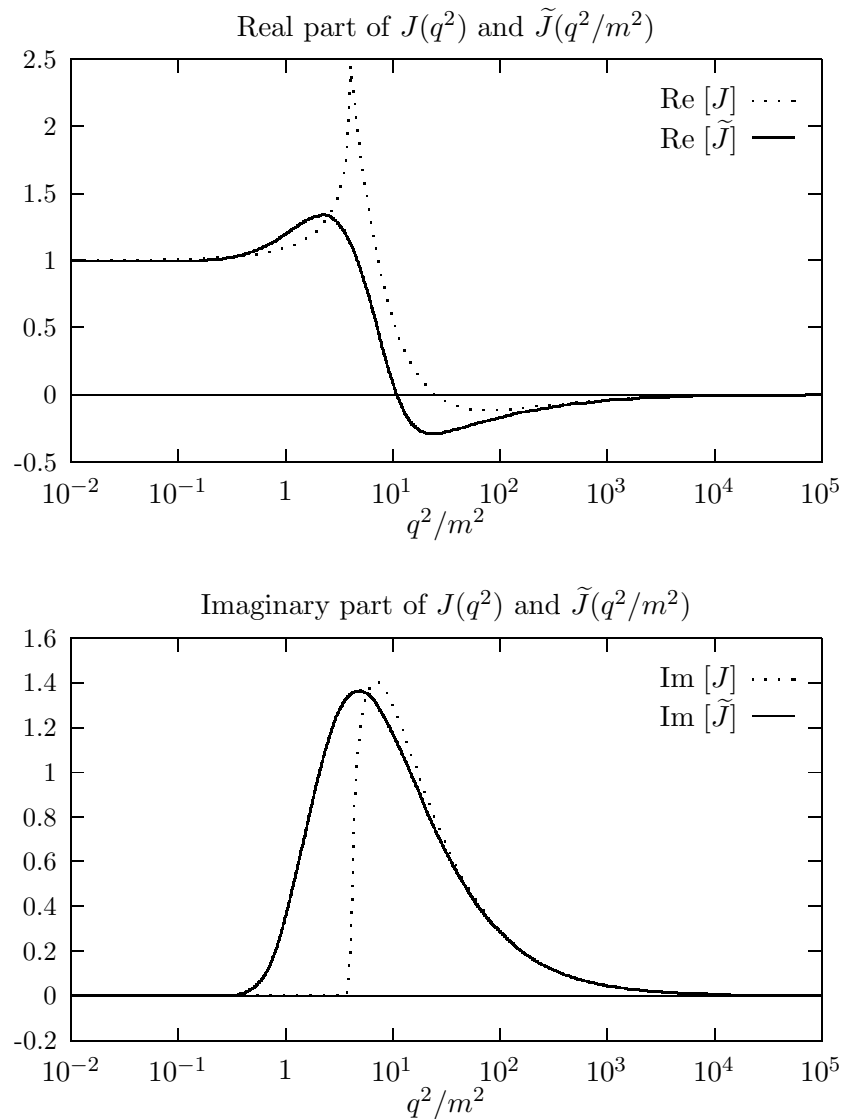


Figure 2: The QCD corrected-improved functions  $\tilde{J}(q^2/m^2)$  (solid lines) comparing with the original functions  $J(q^2)$  (dotted lines), where we take the parameter choice  $\alpha = 1.4$ ,  $\beta = 0.35$  and  $\lambda = 2.5$ .

effective chiral Lagrangian is expressed in terms of two SU(2) matrix valued variables  $\xi_{L,R}(x)$  such that<sup>‡</sup>

$$\xi_L^\dagger(x)\xi_R(x) = e^{2i\pi/f_\pi} (= U(x)), \quad (4.1)$$

from which it is convenient to define the algebra valued (covariantized) 1-form;

$$\begin{aligned} \hat{\alpha}_{\mu\parallel} &= \left( D_\mu \xi_L \cdot \xi_L^\dagger + D_\mu \xi_R \cdot \xi_R^\dagger \right) / 2i, \\ \hat{\alpha}_{\mu\perp} &= \left( D_\mu \xi_L \cdot \xi_L^\dagger - D_\mu \xi_R \cdot \xi_R^\dagger \right) / 2i, \end{aligned} \quad (4.2)$$

with the covariant derivatives defined by

$$\begin{aligned} D_\mu \xi_L &= \partial_\mu \xi_L - igV_\mu \xi_L + ie\xi_L \mathcal{L}, \\ D_\mu \xi_R &= \partial_\mu \xi_R - igV_\mu \xi_R + ie\xi_R \mathcal{R}, \end{aligned} \quad (4.3)$$

where  $V_\mu$  are the vector mesons realized as the hidden local gauge fields:

$$V = \frac{1}{\sqrt{2}} \begin{pmatrix} \frac{1}{\sqrt{2}}(\rho^0 + \omega) & \rho^+ \\ \rho^- & -\frac{1}{\sqrt{2}}(\rho^0 - \omega) \end{pmatrix}, \quad (4.4)$$

$\mathcal{L}$  and  $\mathcal{R}$  denote the external gauge field,  $g$  the hidden local gauge coupling and  $e$  the electromagnetic coupling constant. The external fields are rewritten into the electroweak gauge fields,  $\mathcal{B}$  (photon),  $Z$  and  $W$ :

$$\begin{aligned} \mathcal{L}_\mu &= Q [\mathcal{B}_\mu - \tan\theta_W \mathcal{Z}_\mu] + \frac{1}{\sin\theta_W \cos\theta_W} T_z \cdot \mathcal{Z}_\mu + \frac{1}{\sqrt{2}\sin\theta_W} \mathcal{W}_\mu, \\ \mathcal{R}_\mu &= Q [\mathcal{B}_\mu - \tan\theta_W \mathcal{Z}_\mu], \end{aligned} \quad (4.5)$$

with

$$\mathcal{W}_\mu = \begin{pmatrix} 0 & \mathcal{W}_\mu^+ \cos\theta_C \\ \mathcal{W}_\mu^- \cos\theta_C & 0 \end{pmatrix}, \quad (4.6)$$

$$Q = \frac{1}{3} \begin{pmatrix} 2 & 0 \\ 0 & -1 \end{pmatrix}, \quad T_z = \frac{1}{2} \begin{pmatrix} 1 & 0 \\ 0 & -1 \end{pmatrix}, \quad (4.7)$$

where  $\theta_W$  and  $\theta_C$  are the Weinberg and Cabibbo angles, respectively.

Since  $\hat{\alpha}_{\mu\parallel}$  and  $\hat{\alpha}_{\mu\perp}$  transform as

$$\hat{\alpha}_{\mu\parallel,\perp}(x) \rightarrow h(x)\hat{\alpha}_{\mu\parallel,\perp}(x)h^\dagger(x), \quad (4.8)$$

---

<sup>‡</sup>To be exact, we have to consider the  $[U(3)_L \times U(3)_R]_{\text{global}} \times [U(3)_V]_{\text{hidden}}$  model[14], which contains the nonet vector mesons  $\rho$ ,  $K^*$ ,  $\bar{K}^*$ ,  $\omega$  and  $\phi$ . We only write the part concerning to the  $\pi$  for reasons of mathematical simplicity, hereafter.

where  $h(x)$  is an element of the hidden local gauge group, the Lagrangian is given by[6]

$$\begin{aligned}\mathcal{L}_0 &= \mathcal{L}_A + a\mathcal{L}_V + \mathcal{L}_{\text{kin}}(V_\mu), \\ \mathcal{L}_V &= f_\pi^2 \text{tr} \langle (\hat{\alpha}_{\mu\parallel})^2 \rangle, \quad \mathcal{L}_A = f_\pi^2 \text{tr} \langle (\hat{\alpha}_{\mu\perp})^2 \rangle,\end{aligned}\quad (4.9)$$

where  $a$  is an arbitrary parameter to be determined from experiment. Experimentally, in the real QCD system the hidden local gauge coupling is found to be<sup>§</sup>

$$\frac{g^2}{4\pi} = 2.7 \sim 3.0. \quad (4.10)$$

From the Lagrangian, Eq.(4.9), we get the  $VV$  mixing ( $\mathcal{V}_\mu \equiv (\mathcal{R}_\mu + \mathcal{L}_\mu)/2$ ) as

$$\begin{aligned}\mathcal{L}_{VV} &= -2eg_\rho \text{tr} \langle V_\mu \mathcal{V}^\mu \rangle \\ &= -e \left[ \mathcal{B}^\mu \left\{ g_\rho \rho_\mu^0 + g_\omega \omega_\mu \right\} + \mathcal{Z}^\mu \left\{ g_{Z\rho} \rho_\mu^0 + g_{Z\omega} \omega_\mu \right\} + \dots \right],\end{aligned}\quad (4.11)$$

where

$$g_\rho = 3g_\omega = agf_\pi^2, \quad g_{Z\rho} = \frac{1 - 2 \sin^2 \theta_W}{2 \sin \theta_W \cos \theta_W} g_\rho, \quad g_{Z\omega} = -\frac{\sin \theta_W}{3 \cos \theta_W} g_\rho. \quad (4.12)$$

## 4.2 Hidden Local Symmetry with Anomaly Terms

This framework of HLS provides us with the easiest way to incorporate the vector mesons consistently with the non-abelian anomaly. Following Ref.[6, 12], we introduce the non-abelian anomaly into the HLS model. The general solution to the Wess-Zumino anomaly equation[1] possessing HLS is given by

$$\Gamma \left[ \xi_L^\dagger \xi_R, V, \mathcal{L}, \mathcal{R} \right] = \Gamma_{WZ} \left[ \xi_L^\dagger \xi_R, \mathcal{L}, \mathcal{R} \right] + \int_{M^4} \sum_{i=1}^4 c_i \mathcal{L}_i, \quad (4.13)$$

where  $\Gamma_{WZ}$  denotes the Wess-Zumino term[1, 2],  $c_i$  are arbitrary constants and  $\mathcal{L}_i$  are the gauge invariant 4-forms which conserve parity and charge conjugation but violate intrinsic parity<sup>¶</sup>:

$$\begin{aligned}\mathcal{L}_1 &= i \text{tr} \langle \hat{\alpha}_L^3 \hat{\alpha}_R - \hat{\alpha}_R^3 \hat{\alpha}_L \rangle, \quad \mathcal{L}_2 = i \text{tr} \langle \hat{\alpha}_L \hat{\alpha}_R \hat{\alpha}_L \hat{\alpha}_R \rangle, \\ \mathcal{L}_3 &= \text{tr} \langle F_V (\hat{\alpha}_L \hat{\alpha}_R - \hat{\alpha}_R \hat{\alpha}_L) \rangle, \quad \mathcal{L}_4 = \text{tr} \langle \hat{F}_L \hat{\alpha}_L \hat{\alpha}_R - \hat{F}_R \hat{\alpha}_R \hat{\alpha}_L \rangle,\end{aligned}\quad (4.14)$$

---

<sup>§</sup>The upper (lower) value corresponds to  $a = 2$  (2.2). The parameter choice  $a = 2$  reproduces[13] the complete  $\rho$  meson dominance for the electromagnetic form factor of the pion[15].

<sup>¶</sup>The intrinsic parity of a particle is defined to be even if its parity equals  $(-1)^{\text{spin}}$ , and odd otherwise[12].

where the gauge covariant building blocks are given by

$$\begin{aligned}\hat{\alpha}_{L,R} &\equiv \frac{1}{i} D\xi_{L,R} \cdot \xi_{L,R}^\dagger = \frac{1}{i} D_\mu \xi_{L,R} \cdot \xi_{L,R}^\dagger dx^\mu, \\ F_V &\equiv g(dV - igV^2), \\ \hat{F}_{L,R} &= \xi_{L,R} F_{L,R} \xi_{L,R}^\dagger, \quad F_L = e(d\mathcal{L} - ie\mathcal{L}^2), \quad F_R = e(d\mathcal{R} - ie\mathcal{R}^2).\end{aligned}\quad (4.15)$$

From Eq.(4.13) we find the  $VV\pi$  vertex[12] as

$$\begin{aligned}\mathcal{L}_{VV\pi} &= 2g_{\omega\rho\pi}\varepsilon^{\mu\nu\rho\sigma} \text{tr} \langle \partial_\mu V_\nu \partial_\rho V_\sigma \cdot \pi \rangle \\ &= g_{\omega\rho\pi}\varepsilon^{\mu\nu\rho\sigma} \left[ \partial_\mu \omega_\nu \partial_\rho \rho_\sigma \cdot \pi + \dots \right],\end{aligned}\quad (4.16)$$

where the coupling constant  $g_{\omega\rho\pi}$  is given by

$$g_{\omega\rho\pi} = -\frac{3g^2}{8\pi^2 f_\pi} c_3. \quad (4.17)$$

Similarly, the  $V\mathcal{V}\pi$  vertex is given by

$$\begin{aligned}\mathcal{L}_{V\mathcal{V}\pi} &= 2g_{\omega\gamma\pi}(c_4 - c_3)\varepsilon^{\mu\nu\rho\sigma} \text{tr} \langle \{\partial_\mu V_\nu, \partial_\rho \mathcal{V}_\sigma\} \cdot \pi \rangle \\ &= g_{\omega\gamma\pi}(c_4 - c_3)\varepsilon^{\mu\nu\rho\sigma} \left[ \partial_\mu \omega_\nu \partial_\rho \mathcal{B}_\sigma \cdot \pi^0 + \frac{1}{3} \partial_\mu \rho_\nu^0 \partial_\rho \mathcal{B}_\sigma \cdot \pi^0 \right. \\ &\quad \left. + \bar{r} \partial_\mu \omega_\nu \partial_\rho \mathcal{Z}_\sigma \cdot \pi^0 - \frac{1}{3} \tan \theta_W \partial_\mu \rho_\nu^0 \partial_\rho \mathcal{Z}_\sigma \cdot \pi^0 + \dots \right],\end{aligned}\quad (4.18)$$

where the coupling constant  $g_{\omega\gamma\pi}$  and  $\bar{r}$  are given by

$$g_{\omega\gamma\pi} = -\frac{3eg}{16\pi^2 f_\pi}, \quad \bar{r} \equiv \frac{1 - 2 \sin^2 \theta_W}{2 \sin \theta_W \cos \theta_W}. \quad (4.19)$$

Moreover, the  $\mathcal{V}\mathcal{V}\pi$  vertex is given by

$$\begin{aligned}\mathcal{L}_{\mathcal{V}\mathcal{V}\pi} &= 3g_{\gamma\gamma\pi}(1 - c_4)\varepsilon^{\mu\nu\rho\sigma} \text{tr} \langle \partial_\mu \mathcal{V}_\nu \partial_\rho \mathcal{V}_\sigma \cdot \pi \rangle \\ &= \frac{1}{2} g_{\gamma\gamma\pi}(1 - c_4)\varepsilon^{\mu\nu\rho\sigma} \left[ \partial_\mu \mathcal{B}_\nu \partial_\rho \mathcal{B}_\sigma \cdot \pi^0 + r \partial_\mu \mathcal{B}_\nu \partial_\rho \mathcal{Z}_\sigma \cdot \pi^0 + \dots \right],\end{aligned}\quad (4.20)$$

where

$$g_{\gamma\gamma\pi} = -\frac{e^2}{4\pi^2 f_\pi}, \quad r \equiv \frac{1 - 4 \sin^2 \theta_W}{2 \sin \theta_W \cos \theta_W}. \quad (4.21)$$

### 4.3 Transition Form Factors Based on Hidden Local Symmetry

Now, the total Lagrangian is given by

$$\begin{aligned}\mathcal{L} &= \mathcal{L}_0 + \mathcal{L}_{WZ} + \sum_{i=1}^4 c_i \mathcal{L}_i \\ &= \mathcal{L}_0 + \mathcal{L}_{\mathcal{V}\mathcal{V}\pi} + \mathcal{L}_{V\mathcal{V}\pi} + \mathcal{L}_{VV\pi} + \dots,\end{aligned}\quad (4.22)$$

and we can write down the various transition form factors using this Lagrangian. The  $\pi^0\gamma^*\gamma^*$  transition form factor is given by

$$\begin{aligned} F^{(\text{HLS})}(\pi^0; \gamma(p^2); \gamma(q^2)) &= (1 - c_4) \\ &+ \frac{c_4 - c_3}{4} \{ D_\rho(p^2) + D_\rho(q^2) + D_\omega(p^2) + D_\omega(q^2) \} \\ &+ \frac{c_3}{2} \{ D_\rho(p^2)D_\omega(q^2) + D_\rho(q^2)D_\omega(p^2) \}, \end{aligned} \quad (4.23)$$

where  $D_\rho(p^2)$  and  $D_\omega(p^2)$  are the Breit-Wigner type propagators for  $\rho$  and  $\omega$  mesons:

$$D_\rho(p^2) = \frac{m_\rho^2}{m_\rho^2 - p^2 - i\sqrt{p^2}\Gamma_\rho}, \quad (4.24)$$

$$D_\omega(p^2) = \frac{m_\omega^2}{m_\omega^2 - p^2 - i\sqrt{p^2}\Gamma_\omega}, \quad (4.25)$$

with  $\Gamma_\rho$  and  $\Gamma_\omega$  being the widths of  $\rho$  and  $\omega$  mesons, respectively. If we set one photon on its mass-shell ( $p^2 = 0$ ), this reduces to

$$\begin{aligned} F^{(\text{HLS})}(\pi^0; \gamma(p^2 = 0); \gamma(q^2)) &= \left(1 - \frac{c_3 + c_4}{2}\right) \\ &+ \frac{c_4 + c_3}{4} \{ D_\rho(q^2) + D_\omega(q^2) \}. \end{aligned} \quad (4.26)$$

The  $Z\pi^0\gamma$  transition form factor is also given as

$$\begin{aligned} F^{(\text{HLS})}(\pi^0; \gamma(p^2); \mathcal{Z}(q^2)) &= (1 - c_4) \\ &+ \frac{c_4 - c_3}{2} \left\{ \frac{\bar{r}}{r} (D_\rho(q^2) + D_\omega(p^2)) - \frac{\bar{r} - r}{r} (D_\omega(q^2) + D_\rho(p^2)) \right\} \\ &+ c_3 \left\{ \frac{\bar{r}}{r} D_\rho(q^2)D_\omega(p^2) - \frac{\bar{r} - r}{r} D_\omega(q^2)D_\rho(p^2) \right\}, \end{aligned} \quad (4.27)$$

where  $\bar{r}$  and  $r$  are already defined in Eqs.(4.19) and (4.21). For the on-shell photon ( $p^2 = 0$ ), this reduces to

$$\begin{aligned} F^{(\text{HLS})}(\pi^0; \gamma(p^2 = 0); \mathcal{Z}(q^2)) &= \left(1 - \frac{c_3 + c_4}{2}\right) \\ &+ \frac{c_3 + c_4}{2} \left\{ \frac{\bar{r}}{r} D_\rho(q^2) - \frac{(\bar{r} - r)}{r} D_\omega(q^2) \right\}. \end{aligned} \quad (4.28)$$

The  $Z$  into  $\pi^0\gamma$  transition amplitude is obtained by multiplying this form factor by  $g_{Z\gamma\pi}$  (see Eq.(6.3))

$$g_{Z\gamma\pi} \equiv \frac{-re^2}{8\pi^2 f_\pi}. \quad (4.29)$$

For  $p^2 = q^2 = 0$ ,  $D_\rho$  and  $D_\omega$  all reduce to 1. Then the RHS's of Eq.(4.23) and Eq.(4.26) become 1 independently of  $c_3$  and  $c_4$ :

$$F^{(\text{HLS})}(\pi^0; \gamma(p^2 = 0); \gamma(q^2 = 0)) = 1. \quad (4.30)$$

This together with the coefficient factor  $g_{\gamma\gamma\pi}$  of Eq.(4.21), excellently reproduces the experimental value of the  $\pi^0 \rightarrow \gamma\gamma$  process: this is nothing but the expression of the low energy theorem. On the other hand, in the high energy limit, since  $D_\rho$  and  $D_\omega$  are suppressed by order  $1/q^2$ , the constant terms  $(1 - c_4)$  in Eqs.(4.23) and (4.27) and  $1 - (c_3 + c_4)/2$  in Eqs.(4.26) and (4.28) become dominant. We know that these  $q^2$  independent terms necessarily violate the unitarity bound in the high  $q^2$  ( $p^2$ ) limit. Thus it is necessary to modify the form factor of Eqs.(4.27) and (4.28).

## 5 Expression for The Transition Form Factors

In the previous section, we have derived the transition form factors  $F^{(\text{HLS})}$  from the effective chiral Lagrangian based on HLS. The transition form factors  $F^{(\text{HLS})}$  describe the low energy processes induced by the axial anomaly very well. However, as we discussed in the previous section, we can not extend these form factors to the high energy region in their original forms. In this section, we propose a new expression for the transition form factors which are applicable independent of the energy regions. Let us pay attention to the constant anomaly terms appearing in the first terms of the form factors Eqs.(4.23), (4.26), (4.27) and (4.28), which come from  $\mathcal{L}_{\text{WZ}}$  of Eq.(4.22). In the low energy limit, we have seen that the value of this anomaly term is given by calculating the famous triangle anomaly graph of Fig. 1. In sect. 3, we have proposed  $\tilde{J}(q^2)$  as the QCD corrected anomaly amplitudes. We now further propose to use modified form factors where the constant anomaly terms are replaced by the improved ones. The concrete expressions are as follows. The  $\pi^0\gamma^*\gamma^*$  transition form factor is

$$\begin{aligned} F_{\pi^0\gamma^*\gamma^*}(p^2, q^2) &\equiv F(\pi^0, \gamma(p^2), \gamma(q^2)) \\ &= (1 - c_4)\tilde{I}(p^2, q^2) \\ &\quad + \frac{c_4 - c_3}{4} \left[ \{D_\rho(p^2) + D_\omega(p^2)\} \tilde{J}(q^2) + \{D_\rho(q^2) + D_\omega(q^2)\} \tilde{J}(p^2) \right] \\ &\quad + \frac{c_3}{2} [D_\rho(p^2)D_\omega(q^2) + D_\rho(q^2)D_\omega(p^2)], \end{aligned} \quad (5.1)$$

in which the constant anomaly terms  $(1 - c_4)$  and  $\frac{c_4 - c_3}{4}$  of Eq.(4.23) have been replaced by the smeared functions  $(1 - c_4)\tilde{I}^\parallel$  and  $\frac{c_4 - c_3}{4}\tilde{J}$ , respectively.

As expected, this form factor again satisfies the low energy theorem:

$$F(\pi^0, \gamma(p^2 = 0), \gamma(q^2 = 0)) = 1, \quad (5.2)$$

---

<sup>||</sup>The function  $\tilde{I}$  is obtained by the same procedure as  $\tilde{J}$ .

which is independent of the parameters  $c_3$  and  $c_4$ . In the high energy region, on the other hand, we have  $D_\rho(q^2) \sim m_\rho^2/q^2$  and  $D_\omega(q^2) \sim m_\omega^2/q^2$ . If one notices that  $m_\rho \sim m_\omega \sim \mathcal{O}(f_\pi)$ , it is easy to see that  $\rho$  and  $\omega$  pole contributions have the same high energy properties as  $\tilde{I}$  and  $\tilde{J}$ .

In much the same way we have

$$\begin{aligned} F_{\pi^0\gamma}(q^2) &\equiv F\left(\pi^0, \gamma(p^2 = 0), \gamma(q^2)\right) \\ &= \left(1 - \frac{c_3 + c_4}{2}\right) \tilde{J}(q^2) + \frac{c_3 + c_4}{4} \left\{D_\rho(q^2) + D_\omega(q^2)\right\}, \end{aligned} \quad (5.3)$$

$$\begin{aligned} F_{\pi^0\gamma^*Z^*}(p^2, q^2) &\equiv F\left(\pi^0; \gamma(p, \mu); \mathcal{Z}(q, \nu)\right) \\ &= (1 - c_4) \tilde{I}(p^2, q^2) \\ &\quad + \frac{c_4 - c_3}{2} \left\{ \frac{\bar{r}}{r} \left( D_\rho(q^2) \tilde{J}(p^2) + D_\omega(p^2) \tilde{J}(q^2) \right) \right. \\ &\quad \left. - \frac{\bar{r} - r}{r} \left( D_\omega(q^2) \tilde{J}(p^2) + D_\rho(p^2) \tilde{J}(q^2) \right) \right\} \\ &\quad + c_3 \left\{ \frac{\bar{r}}{r} D_\rho(q^2) D_\omega(p^2) - \frac{\bar{r} - r}{r} D_\rho(p^2) D_\omega(q^2) \right\}, \end{aligned} \quad (5.4)$$

$$\begin{aligned} F_{Z\pi^0\gamma}(q^2) &\equiv F\left(\pi^0, \gamma(p^2 = 0), Z(q^2)\right) \\ &= \left(1 - \frac{c_3 + c_4}{2}\right) \tilde{J}(q^2) + \frac{c_3 + c_4}{2} \left\{ \frac{\bar{r}}{r} D_\rho(q^2) - \frac{\bar{r} - r}{r} D_\omega(q^2) \right\}, \end{aligned} \quad (5.5)$$

where  $\bar{r}$  and  $r$  are defined in Eqs.(4.19) and (4.21).

The vector meson form factors can also be obtained. For the later convenience we give the expression for the  $\omega\pi^0$  transition form factor. By extracting the  $\omega$ -pole contributions from Eq.(5.1) and by making proper normalization of the amplitude we find

$$F_\omega(q^2) = -\tilde{c} \tilde{J}(q^2) + (1 + \tilde{c}) D_\rho(q^2), \quad \tilde{c} \equiv \frac{c_3 - c_4}{c_3 + c_4}. \quad (5.6)$$

In the following sections, we compare the above formulae with the experimental data. In doing this, it is important to bear in mind the following two points:

- 1) The complete vector meson dominance (VMD) hypothesis

Since the proposal of the VMD model[15], it has often been believed that VMD never led to contradictions with the experimental data, and in many analyses VMD was taken for granted. We should stress here that all the processes so far examined are those which occur in either the low energy or the high energy limit. As may be seen from the expressions for the form factors derived in this section, realization of the VMD hypothesis depends on the parameters  $c_i$  ( $c_3$  and  $c_4$  in our case). As we have already mentioned, in the low and high energy limits the results are independent of

the choice of these parameter. For example,  $\Gamma(\pi^0 \rightarrow \gamma\gamma)$  can be evaluated correctly either from the pure Wess-Zumino term or by using the VMD hypothesis. The results are found to coincide completely. In the high energy limit, on the other hand, Arnellos et al.[16] pointed out that the  $\rho$  meson dominant form factor gives the correct high energy behavior. So we should remark that it is the intermediate energy phenomena which determine the parameters  $c_i$ .

So, the question is in what experimental process we can observe the deviation from the complete VMD hypothesis, in which the triangle anomaly terms are appreciable.

## 2) Constant versus momentum dependent triangle anomaly terms

If nature is described by the VMD model, the triangle anomaly term does not contribute either to the form factors or to the decay amplitudes: for example, the parameter choice  $c_3 = c_4 = 1$  in our form factor corresponds to VMD:

$$F_{\pi^0\gamma^*\gamma^*}(p^2, q^2) = \frac{1}{2} [D_\rho(p^2)D_\omega(q^2) + D_\rho(q^2)D_\omega(p^2)], \quad (5.7)$$

and in this case the  $\tilde{I}$  and  $\tilde{J}$  terms disappear. However, as we shall see below, complete VMD is not always realized in nature, so we need the information from the triangle anomaly terms. For the low  $q^2$  region, most of the analyses use the amplitude obtained directly from the Wess-Zumino term[1, 2]. Namely, they adopt the form factors  $F^{(\text{HLS})}$  of section 4. For example, Bramon et al.[17] have made an extensive analysis for relatively high  $q^2$  region using  $F^{(\text{HLS})}$ .

If we further straightforwardly extend the amplitudes  $F^{(\text{HLS})}$  to the higher  $q^2$  region, say, for example,  $q^2 = M_Z^2$ , we would get an extraordinary large decay amplitude for  $Z \rightarrow \pi^0\gamma$ [18]. There have been many discussions concerning this process (see, for example, Refs. [9], [10] and [11]), which have made it clear that the form factor should be strongly suppressed.

Our interest here is in examining intermediate  $q^2$  phenomena to see how the anomaly term depends on  $q^2$ .

## 6 $\pi^0\gamma\gamma^*$ Process

In this section we apply our form factors of the previous section to the  $\pi^0\gamma$  transition form factor and also to the  $Z \rightarrow \pi^0\gamma$  decay.

## 6.1 $\pi^0\gamma$ Transition Form Factor

The  $\pi^0\gamma$  transition form factor is given in Eq.(5.3);

$$F_{\pi^0\gamma}(q^2) = \left(1 - \frac{c_3 + c_4}{2}\right) \tilde{J}(q^2) + \frac{c_3 + c_4}{4} \left\{D_\rho(q^2) + D_\omega(q^2)\right\}, \quad (6.1)$$

in which  $(c_3 + c_4)/2$  is to be determined from the experimental data[19]. The experimental data points are shown in Fig. 3, together with these theoretical curves. The thick line corresponds to the VMD:

$$\frac{c_3 + c_4}{2} = 1.0, \quad (6.2)$$

and the thin (dotted) line corresponds to a 5% increase (decrease) in this value. The result indicates that the VMD is almost realized in this process.

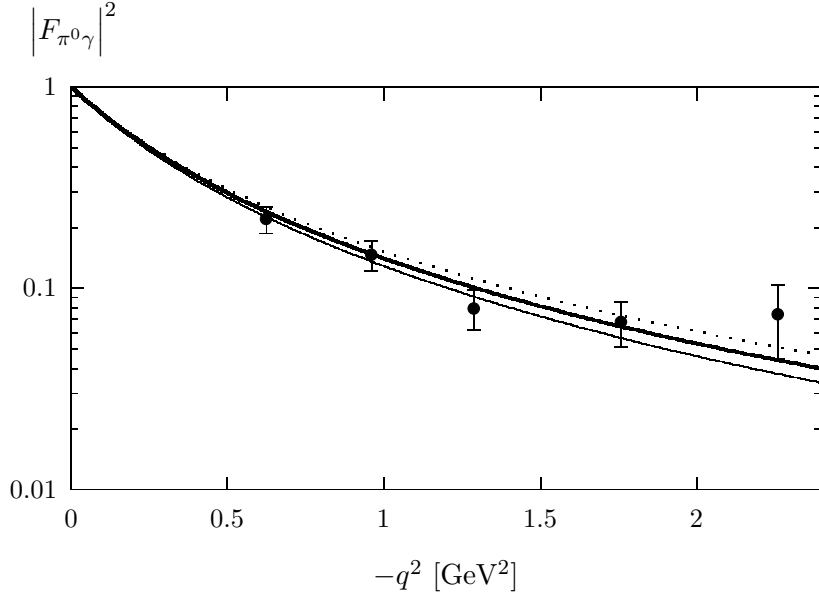


Figure 3: The  $\pi^0\gamma$  transition form factor, where the dotted line corresponds to the parameter choice  $(c_3 + c_4)/2 = 0.95$ , the thick line,  $(c_3 + c_4)/2 = 1.0$  (VMD) and the thin line,  $(c_3 + c_4)/2 = 1.05$ , respectively.

## 6.2 $Z \rightarrow \pi^0\gamma$ Decay

By extrapolating the form factor  $F_{Z\pi^0\gamma}(q^2)$  of Eq.(5.5) to  $q^2 = M_Z^2$ , we obtain the decay width  $\Gamma(Z \rightarrow \pi^0\gamma)$  together with the coefficient factor  $g_{Z\gamma\pi}$  of Eq.(4.29):

$$\Gamma(Z \rightarrow \pi^0\gamma) = \frac{\alpha^2 r^2}{48\pi^3 f_\pi^2} \left| \frac{M_Z^2 - m_\pi^2}{2M_Z} \right|^3 \left| F_{Z\pi^0\gamma}(q^2 = M_Z^2) \right|^2. \quad (6.3)$$

We have already seen that the parameter  $(c_3 + c_4)/2$  is almost equal to 1, so the first term of Eq.(5.5) which is proportional to  $\tilde{J}$  does not contribute to the decay width. We therefore obtain

$$\Gamma(Z \rightarrow \pi^0\gamma) = 0.8 \times 10^{-11} \quad (\text{GeV}), \quad (6.4)$$

which is of roughly the same order as has been predicted by other authors[8, 9, 10, 11, 16].

## 7 Application to $\omega$ Process

The  $\omega\pi^0$  transition form factor is given by Eq.(5.6):

$$F_\omega(q^2) = -\tilde{c}\tilde{J}(q^2) + (1 + \tilde{c})D_\rho(q^2), \quad \tilde{c} \equiv \frac{c_3 - c_4}{c_3 + c_4}. \quad (7.1)$$

where  $\tilde{c}$  is to be determined. We compare the above improved form factor with the following unimproved form factor:

$$F_\omega^C(q^2) = -\tilde{c} + (1 + \tilde{c})D_\rho(q^2), \quad (7.2)$$

in which the triangle anomaly term is taken to be a constant.

### 7.1 $\omega \rightarrow \pi^0\gamma$ Decay

First, we study the  $\omega \rightarrow \pi^0\gamma$  decay. Since all the external fields are on mass shell, the form factor reduces to 1, and the decay width is given by

$$\Gamma(\omega \rightarrow \pi^0\gamma) = \left(\frac{1}{2}(c_3 + c_4)g\right)^2 \frac{3\alpha}{64\pi^4 f_\pi^2} \left|\frac{m_\omega^2 - m_\pi^2}{2m_\omega}\right|^3, \quad (7.3)$$

where  $g$  is the gauge coupling constant of the hidden local gauge boson.

From the experimental data[20]

$$\Gamma(\omega \rightarrow \pi^0\gamma)/\Gamma_\omega = (8.5 \pm 0.5) \times 10^{-2}, \quad (7.4)$$

or

$$\Gamma(\omega \rightarrow \pi^0\gamma)_{\text{exp}} = (7.2 \pm 0.5) \times 10^{-1} \quad (\text{MeV}), \quad (7.5)$$

and so we find

$$\left(\frac{1}{2}(c_3 + c_4)g\right)^2 = 32.6 \pm 2.3. \quad (7.6)$$

Using the value of  $g$  given in Eq.(4.10) we get

$$\frac{1}{2}(c_3 + c_4) = 0.90 \sim 1.0, \quad (7.7)$$

which is to be compared with the value we independently derived in sect. 6.1 (see Eq.(6.2)). Thus HLS also describes the  $\omega \rightarrow \pi^0\gamma$  decay well[12]. In the form factor analysis below, we take the  $\omega \rightarrow \pi^0\gamma$  decay width as an input.

## 7.2 $\omega \rightarrow \pi^0 \mu^+ \mu^-$ Decay

We now consider the  $\omega \rightarrow \pi^0 \mu^+ \mu^-$  decay. This gives information about the form factor at high  $q^2$ . It is convenient to write this decay width as[21]

$$\begin{aligned} \Gamma(\omega \rightarrow \pi^0 \mu^+ \mu^-) &= \int_{4m_\mu^2}^{(m_\omega - m_\pi)^2} dq^2 \frac{\alpha}{3\pi} \frac{\Gamma(\omega \rightarrow \pi^0 \gamma)}{q^2} \left(1 + \frac{2m_\mu^2}{q^2}\right) \sqrt{\frac{q^2 - 4m_\mu^2}{q^2}} \\ &\times \left[ \left(1 + \frac{q^2}{m_\omega^2 - m_\pi^2}\right)^2 - \frac{4m_\omega^2 q^2}{(m_\omega^2 - m_\pi^2)^2} \right]^{3/2} |F_\omega(q^2)|^2, \end{aligned} \quad (7.8)$$

where  $q^2$  is the intermediate photon momentum (or invariant mass of final muons), and  $F_\omega(q^2)$  is the  $\omega \pi^0$  transition form factor given in Eq.(7.1).

We find

$$\Gamma(\omega \rightarrow \pi^0 \mu^+ \mu^-) = (8.97 + 1.79\tilde{c} + 0.32\tilde{c}^2) \times 10^{-4} \times \Gamma(\omega \rightarrow \pi^0 \gamma) \quad (\text{MeV}). \quad (7.9)$$

The experimental value for the branching ratio of this mode is given by[20]

$$\Gamma(\omega \rightarrow \pi^0 \mu^+ \mu^-)/\Gamma\omega = (9.6 \pm 2.3) \times 10^{-5}, \quad (7.10)$$

and using this and the branching ratio of  $\omega \rightarrow \pi^0 \gamma$  in Eq.(7.4), we find

$$\frac{\Gamma(\omega \rightarrow \pi^0 \mu^+ \mu^-)}{\Gamma(\omega \rightarrow \pi^0 \gamma)} = \frac{(9.6 \pm 2.3) \times 10^{-5}}{(8.5 \pm 0.5) \times 10^{-2}} \simeq (1.1 \pm 0.3) \times 10^{-3}. \quad (7.11)$$

From these we obtain\*\*

$$\tilde{c} = 0.49^{+0.12}_{-0.13}. \quad (7.12)$$

This clearly shows that complete  $\rho$  meson dominance is incapable of describing the  $\omega \pi^0$  form factor[21] (VMD corresponds to  $\tilde{c} = 0$ , see Eq.(7.1)).

## 8 Overall Fit of Form Factor

As we saw in the previous section, the transition form factor  $\omega \rightarrow \pi^0 \gamma$  receives appreciable contributions from the anomaly term, and we use this process to obtain information about the  $q^2$  dependence from the experimental data. The available experimental data for  $\omega \pi^0 \gamma^*$  lies in a relatively wide energy range (up to 1.4GeV). We compare our form factor  $F_\omega$  with the unimproved form factor  $F_\omega^C$ .

---

\*\*The another solution  $\tilde{c} = -2.5 \pm 0.1$  is excluded by experiments.

## 8.1 $\omega\pi^0$ Transition Form Factor below $m_\omega$

First, we fit our form factor given in Eq.(7.1) to the experimental data [21]. In the very low energy region the function  $\tilde{J}(q^2)$  is approximately 1 and so  $q^2$  dependent effects are very small. The results are shown in Fig. 4, in which the thick line corresponds to the parameter choice  $\tilde{c} = 1$ , the thin line,  $\tilde{c} = 0.5$  and the dotted line,  $\tilde{c} = 0$  (VMD).

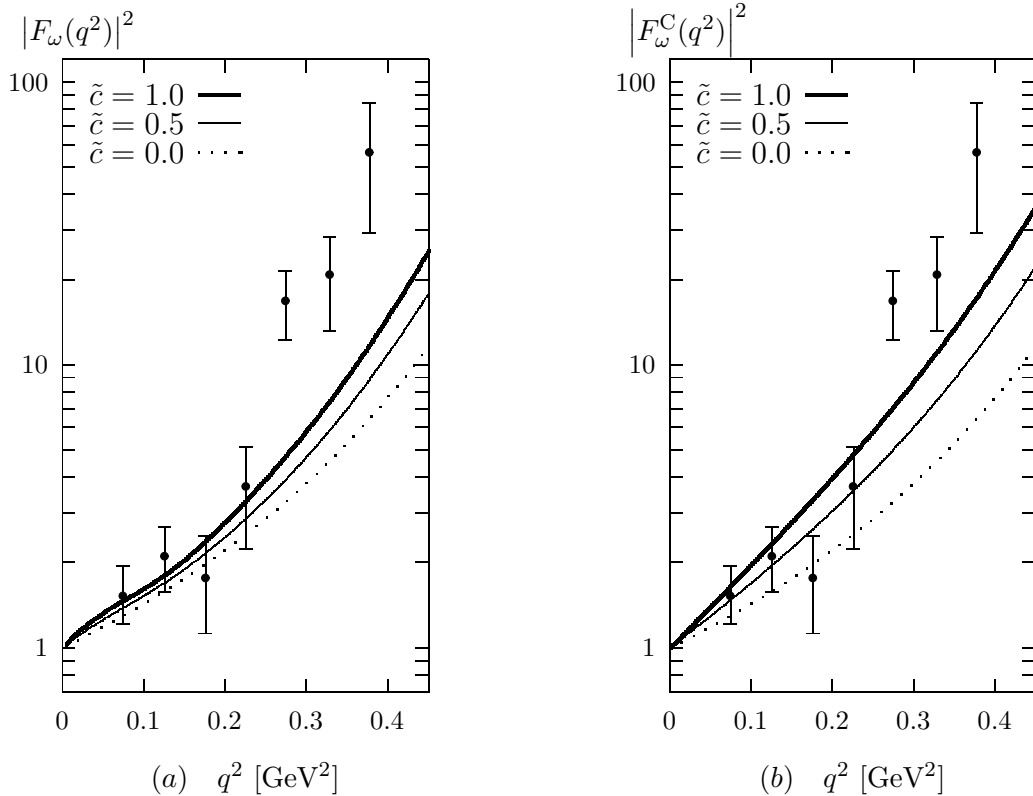


Figure 4: The  $\omega\pi^0$  transition form factor in the energy range below  $m_\omega$ : (a) our form factor  $F_\omega(q^2)$ ; (b) unimproved form factor  $F_\omega^C(q^2)$ . We use the experimental data shown in Ref.[21]. In (a) and (b), the thick line corresponds to the parameter choice  $\tilde{c} = 1$ , the thin line,  $\tilde{c} = 0.5$  and the dotted line,  $\tilde{c} = 0$  (VMD).

Although the experimental data shows some deviation from the theoretical curve, we can clearly exclude the VMD value  $\tilde{c} \simeq 0$ . A rough estimate gives<sup>††</sup>

$$\tilde{c} = 0.5 \sim 1.0, \quad (8.1)$$

<sup>††</sup>In Ref. [17], the value  $\tilde{c} = 0.5$  is used.

which is to be compared with Eq.(7.12). So far as we only use the low energy data, we can not clearly discriminate between our form factor  $F_\omega$  and the unimproved one  $F^C$ .

## 8.2 $e^-e^+ \rightarrow \omega\pi^0$

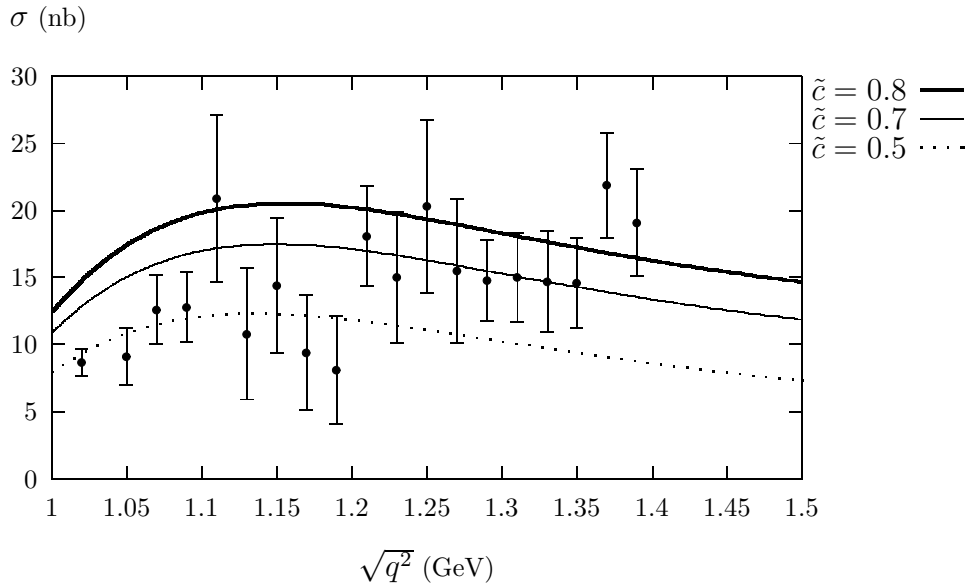


Figure 5: Total cross section of the process  $e^-e^+ \rightarrow \omega\pi^0$  in the energy region from 1 GeV to 1.4 GeV using our form factor  $F_\omega(q^2)$ . The thick line corresponds to the parameter choice  $\tilde{c} = 0.8$ , the thin line,  $\tilde{c} = 0.7$  and the dotted line,  $\tilde{c} = 0.5$ . The experimental data is given in Ref.[22].

Let us go to the higher  $q^2$  region and study the process  $e^-e^+ \rightarrow \omega\pi^0$ . In this case  $q^2$  is the total energy squared of the  $e^+e^-$  pair ( $q^2 > (m_\omega + m_\pi)^2$ ). The cross section for  $e^-e^+ \rightarrow \omega\pi^0$  is given by

$$\sigma(e^-e^+ \rightarrow \omega\pi^0) = 4\pi\alpha\Gamma(\omega \rightarrow \pi^0\gamma) \frac{q^2 + 2m_e^2}{q^4\sqrt{q^2 - 4m_e^2}} \frac{p_\omega^3(q^2)}{p_\gamma^3} \times |F_\omega(q^2)|^2, \quad (8.2)$$

where  $p_\omega(q^2)$  and  $p_\gamma$  denote the  $\omega$  momentum and the photon momentum respectively. These are given by

$$p_\gamma = \frac{m_\omega^2 - m_\pi^2}{2m_\omega}, \quad (8.3)$$

$$p_\omega(q^2) = \frac{1}{2\sqrt{q^2}} \sqrt{(q^2 - (m_\omega + m_\pi)^2)(q^2 - (m_\omega - m_\pi)^2)}. \quad (8.4)$$

The results using our form factor  $F_\omega$  are shown in Fig. 5, from which we find that the effect of the function  $\tilde{J}(q^2)$  suppresses the cross section appreciably. This enables us to reproduce the experimental data with the value  $\tilde{c} = 0.5 \sim 0.8$ . On the other hand, the predictions using the unimproved form factor  $F_\omega^C$  (see Fig. 6) prefer the value  $\tilde{c} = 0.25 \sim 0.40$ , which is smaller than that of Eq.(8.1).

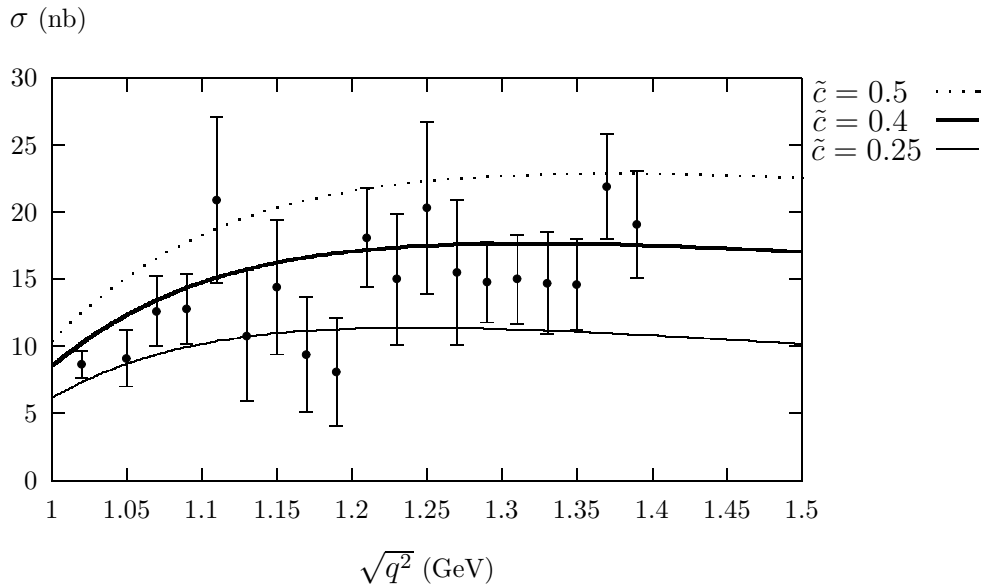


Figure 6: Total cross section of the process  $e^-e^+ \rightarrow \omega\pi^0$  in the energy region from 1 GeV to 1.4 GeV using the unimproved form factor  $F_\omega^C(q^2)$ . The thick line corresponds to the parameter choice  $\tilde{c} = 0.4$ , the thin line,  $\tilde{c} = 0.25$  and the dotted line,  $\tilde{c} = 0.5$ . The experimental data is given in Ref.[22].

### 8.3 Overall Fit in the Energy Range below 1.4 GeV

To summarizing the result so far examined: Data for the  $\pi^0\gamma$  transition form factor indicates that  $(c_3 + c_4)/2 = 1$ , and so their experiment is consistent with VMD. It must be noted, however, that VMD of  $\pi^0\gamma$  transition form factor does not imply  $c_3 = c_4 = 1$ . In fact, the experimental data for the  $\omega\pi^0$  transition form factor shows  $\tilde{c} \neq 0$  ( $\tilde{c} = 0.5 \sim 0.8$ ), i.e.,  $c_3 \neq c_4$ , which implies some deviation from VMD. Bearing these facts in mind we here study our form factor  $F_\omega$  by comparing it with the experimental data over the whole energy range below 1.4 GeV. To do this, it is convenient to convert the cross section data of Fig. 5 into values for the form factor, and combine the result with the values of Fig. 4.

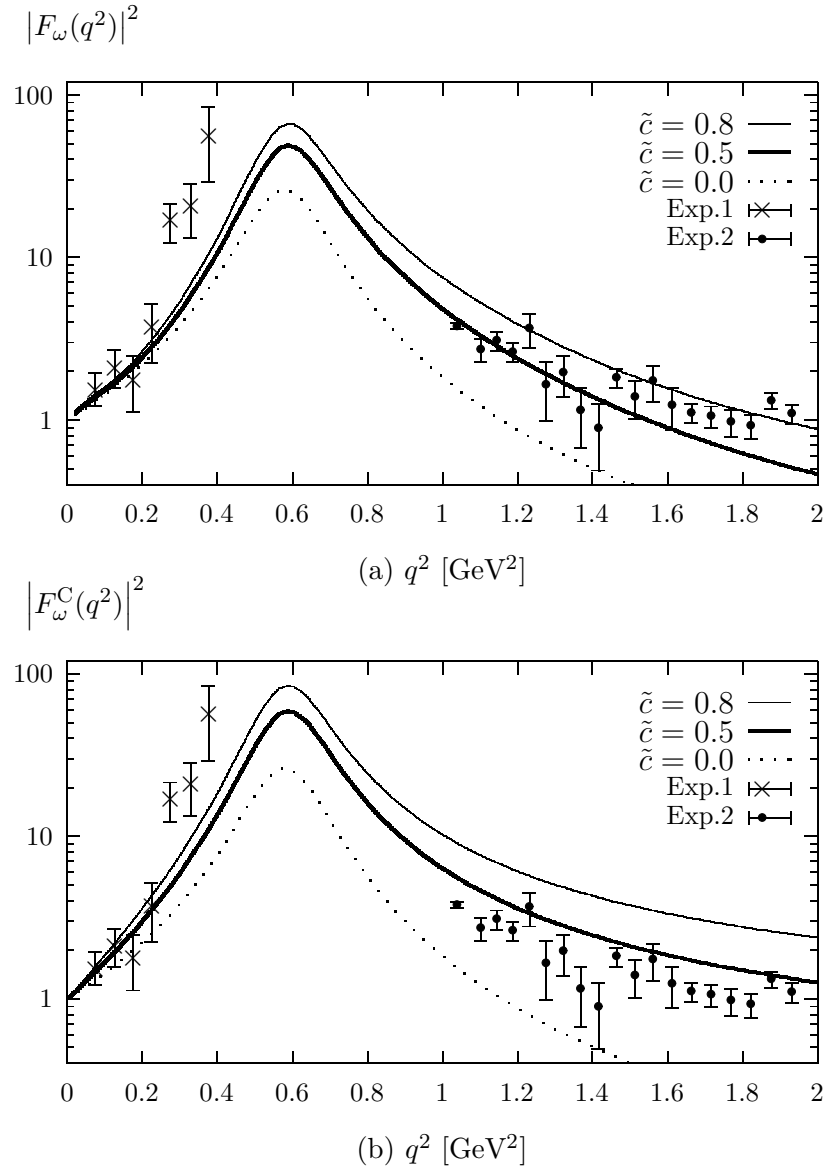


Figure 7: The form factor in the energy range below 1.4 GeV. The low energy data (Exp.1) is given in Ref.[21], and the high energy data (Exp.2) is translated from the cross section data[22]. The thick line ( $\tilde{c} = 0.5$ ), the thin line ( $\tilde{c} = 0.8$ ) and the dotted line ( $\tilde{c} = 0.0$ ) show the values of (a) our form factor  $F_\omega(q^2)$  and (b) unimproved one  $F_\omega^C(q^2)$ .

The predicted curves are shown in Fig. 7. For reference we show the fitting using the unimproved form factor  $F_\omega^C$ .

## 9 Summary and Further Outlook

We have seen that the axial anomaly induced amplitudes are not always expressed in terms of a VMD model. So far as the  $\pi^0\gamma$  transition form factor is concerned, the experiments indicate that VMD works well. On the other hand, in the experiments for  $\omega\pi^0$  form factor, it does not. Because of this deviation from VMD, the anomaly term contributions become important.

It should be remarked that, even for the  $\pi^0\gamma$  transition form factor, there may be cases where the  $q^2$  dependence of the anomaly term becomes important. For example, if we adopt a constant anomaly term, even very small deviation from VMD yields a large  $Z \rightarrow \pi^0\gamma$  decay width: let the deviation from VMD be  $\varepsilon$ , so that  $\frac{c_3+c_4}{2} = 1+\varepsilon$ , and let us suppose that  $\varepsilon$  is very small, say for example,  $10^{-1}$ . Since the suppression of  $D_\rho(q^2) \sim m_\rho^2/M_Z^2$  is of order  $\mathcal{O}(10^{-4})$ , the first term of Eq.(4.28) dominates, which yields  $\Gamma(Z \rightarrow \pi^0\gamma) \sim \mathcal{O}(10^{-5})\text{GeV}$ . The  $10^7$   $Z$  events at LEP then might include the rare decay  $\pi^0\gamma$  events already.

The main task in this paper has been to investigate the  $q^2$  dependence of this anomaly term. We proposed a form factor with the improved triangle anomaly amplitudes  $\tilde{I}$  and  $\tilde{J}$  of Eq.(5.1) and saw that this reproduces the existing  $\omega\pi^0$  form factors (at least up to 1.4 GeV).

This form factor is found to also be consistent with the extremely high  $q^2$  behavior. At present, however, there exists no data to check whether we can extend our form factor to the region  $q^2 > (1.4\text{GeV})^2$ . In this sense the  $Z \rightarrow \pi^0\gamma$  process may be important. Unfortunately in addition to the suppression factor  $\mathcal{O}(f_\pi^2/q^2)$ , the coupling with the  $Z$  is proportional to

$$Q^z = \frac{1}{\sin \theta_W \cos \theta_W} \left[ \frac{1}{2} T_3 - Q \sin^2 \theta_W \right], \quad (9.1)$$

and the ratio of the coefficient  $g_{Z\gamma\pi}^2$  to  $g_{\gamma\gamma\pi}^2$  (see Eqs.(4.29) and (4.21)) is

$$\left( \frac{r}{2} \right)^2 = \left( \frac{1 - 4 \sin^2 \theta_W}{4 \sin \theta_W \cos \theta_W} \right)^2 \simeq 10^{-3}. \quad (9.2)$$

This is why the  $Z \rightarrow \pi^0\gamma$  decay width is predicted very small.

In the future, the  $W \rightarrow \pi\gamma$  decay processes may give important information, because this amplitude are not suppressed. Two photon processes will also provide us with the another important informations on the function  $\tilde{I}$ .

Finally we make comments on the future tasks.

1) We may expect a considerably larger amplitude for the high  $q^2$  region for decays into NG bosons composed of heavy quarks. For example, the decay of  $Z$  into  $\gamma$  and heavy quarkonia may be experimentally detected in the near future. So it is interesting to extend our formula to heavy quark systems. To do this we have to take account of explicit chiral symmetry breaking effects in the HLS framework.

2) A more interesting possibility is to apply our formulae to strong interacting systems other than QCD. For example, technicolor systems may be one of those possibilities. Recently, there have been proposed various types of technicolor-like dynamics whose scales are of the order of several tens of GeV. In such cases, if the technicolor dynamics is of a different type from QCD, one may expect very light vector bound states or relatively small decay constants of the order of a few tens of GeV. Then the axial anomaly induced processes might play an essential role and may be observed as very clear events.

## Acknowledgement

We would like to thank Taichiro Kugo and Nobuhiro Maekawa for stimulating discussions and comments and also Ken-ichi Hikasa for the discussion about the triangle anomaly term. We are also grateful to Mark Mitchard for critical reading of this manuscript.

## References

- [1] J. Wess and B. Zumino, Phys. Lett. **B37**, 95 (1971).
- [2] E. Witten, Nucl. Phys. **B223**, 422 (1983).
- [3] S. Adler, Phys. Rev. **177**, 2426 (1969).
- [4] J.S. Bell and R. Jackiw, Nuovo Cimento **60**, 37 (1969).
- [5] S. Adler and W. Bardeen, Phys. Rev. **182**, 1517 (1969).
- [6] M. Bando, T. Kugo and K. Yamawaki, Phys. Rep. **164**, 217 (1988).
- [7] G. Lepage and S. Brodsky, Phys. Lett. **B87**, 359 (1979).
- [8] B. Guberina, J.H. Kühn, R.D. Peccei and R. Rückl, Nucl. Phys. **B174**, 317 (1980).
- [9] K. Hikasa, Mod. Phys. Lett. **A5**, 1801 (1990).
- [10] N.G. Deshpande, P.B. Pal and F. Olness, Phys. Lett. **B241**, 119 (1990).
- [11] A. Manohar, Phys. Lett. **B244**, 101 (1990).
- [12] T. Fujiwara, T. Kugo, H. Terao, S. Uehara and K. Yamawaki, Prog. Theor. Phys. **73**, 926 (1985).
- [13] M. Bando, T. Kugo, S. Uehara, K. Yamawaki and T. Yanagida, Phys. Rev. Lett. **54**, 1215 (1985).
- [14] M. Bando, T. Kugo and K. Yamawaki, Nucl. Phys. **B259**, 493 (1985).
- [15] J. Sakurai, *Currents and Mesons* (Univ. Chicago Press, Chicago, 1969).
- [16] L. Arnellos, W.J. Marciano and Z. Parsa, Nucl. Phys. **B196**, 378 (1982).
- [17] A. Bramon, A. Grau and G. Pancheri, Phys. Lett. **B277**, 353 (1992).
- [18] M. Jacob and T. Wu, Phys. Lett. **B232**, 529 (1989).
- [19] CELLO Collaboration, Z. Phys. **C49**, 401 (1991).
- [20] Particle Data Group: Review of Particle Properties, Phys. Rev. **D45**, (1992).
- [21] R.I. Dzhelyadin, et al., Phys. Lett. **B102**, 296 (1981).
- [22] S.I. Dolynsky, et al., Phys. Lett. **B174**, 453 (1986).